Atmospheric Research 326 (2025) 108327

Contents lists available at ScienceDirect

Atmospheric Research

journal homepage: www.elsevier.com/locate/atmosres

Wind tunnel experiments of spontaneous and collision-induced breakup of raindrops and model simulations of the impact of breakup on precipitation

Karoline Diehl [a,*], Tobias Jungbluth [a], Alexander Theis [b], Subir K. Mitra [b], Miklós Szakáll [a]

[a] *Institute of Atmospheric Physics, University of Mainz, Germany*
[b] *Max Planck Institute for Chemistry, Mainz, Germany*

ARTICLE INFO

Keywords:
Raindrops
Spontaneous breakup
Collision-induced breakup
Fragment size distribution
Precipitation

ABSTRACT

Experiments were performed at the Mainz vertical wind tunnel where two types of drop breakup were investigated with freely floating drops. Spontaneous breakup under laminar conditions resulted in 5 % breakup events of drops with equivalent diameters between 8 and 13 mm by separating in the center due to strong oscillations in horizontal mode into two nearly equal sized fragments. In a turbulent airflow, several oscillation types mainly in vertical and transverse directions caused significant deformations of the drops, which seemed to promote the coherence of the drops. Collision-induced breakup occurs when two drops collide and break up into several fragments. To fill the gaps of missing drop sizes in earlier measurements, a set of relevant drop pairs with diameters of 4.0 to 5.2 mm and 1.9 to 3.1 mm was investigated. With a mean breakup efficiency of 0.55, approximately half of breakup events resulted in two or three fragments, the other half in the formation of more than 3 up to 9 fragments. The measured fragment size distributions were compared to results from earlier parameterizations so that modifications due to the new data set were identified. Accompanying the experiments, process studies with a 3D cloud model were performed to study the impact of breakup on drop size distributions and precipitation. It was found that breakup reduces the numbers of the largest raindrops, thereby delays the onset of precipitation, possibly reduces total precipitation amounts and changes the local distribution of precipitation. Important parameters in the process studies were the breakup efficiency as well as the fragment numbers and sizes.

1. Introduction

One of the anticipated effects of climate change is an increase of extreme precipitation events (IPCC, 2023). For the description and analysis of precipitation, the drop size distribution in cloud and precipitation processes is fundamental. It serves as base to derive total drop number concentrations and liquid water contents and finally, by using drop terminal velocities, to compute rainfall rates (Pruppacher and Klett, 2010). Furthermore, drop size distributions are crucial parameters for the interpretation of satellite signals as well as in precipitation now- and forecasting by means of weather radar where the radar reflectivity is related to the precipitation rate. Cloud processes that mainly affect the evolution of the drop size spectrum are collisions, followed by bounce, coalescence, or breakup of drops (Testik, 2009). Bounce means that the drops separate again after collision so that the original drop pair is conserved. In case of coalescence, the drops merge and form a larger drop conserving the volume. In contrast, the drops may breakup into several fragments of different sizes, which is referred to as collision-induced breakup. Besides that, large drops may break up spontaneously when they become aerodynamically unstable due to their oscillations. Breakup reduces in particular the numbers of large drops and may, therefore, decrease the speed of rain formation and surface rain rates (Seifert et al., 2005).

Spontaneous breakup occurs when the energy of the natural drop oscillation (Szakáll et al., 2009) exceeds the surface energy of the drop. Especially the increasing amplitude of the naturally occurring horizontal oscillation mode with increasing size might play a key role (Müller et al., 2013). Turbulences in the airflow may also affect spontaneous drop breakup in the way that turbulent eddies pushing the drops around as a whole (unlike shears in lateral direction) could deliver energy to the drop causing significant shape oscillation that would overwhelm the surface tension and cause disintegration of the drop. Early experimental studies in a fall shaft (Fournier d'Albe and Hidayetulla, 1955) and in a simple vertical wind tunnel (Komabayasi et al., 1964) found

* Corresponding author at: Institute of Atmospheric Physics, University of Mainz, 55099 Mainz, Germany.
E-mail address: kdiehl@uni.mainz.de (K. Diehl).

https://doi.org/10.1016/j.atmosres.2025.108327
Received 13 March 2025; Received in revised form 26 May 2025; Accepted 27 June 2025
Available online 28 June 2025

spontaneous breakup for drops larger than 6 to 8 mm equivalent diameter. A small open vertical wind tunnel using a blower and a back pressure plate to enable free suspension of drops was used by Kamra et al. (1991) to study spontaneous breakup of charged and uncharged drops. While the results from the latter confirmed those from earlier studies, the probability of spontaneous breakup was found to increase with increasing charge. Later, Villermaux and Bossa (2009) conducted experiments where water drops were falling against an air jet. They reported that only drops with equivalent diameters smaller than 6 mm survived; however, the question is whether the air jet they used had affected the stability of the drops because of the introduced nonnatural strong small-scale wind shear. In contrast to this finding, Szakáll et al. (2010) observed drops freely floated in the Mainz vertical wind tunnel larger than 6 mm remaining intact.

Experimental studies on collision-induced breakup indicated that the fragment size distributions and the fragment numbers depend on the breakup type; mostly filament, sheet, and disk breakup, rarely crown breakup (Testik, 2009; Testik et al., 2011; Emersic and Connolly, 2011; Szakáll et al., 2014; Lohmann et al., 2016; Szakáll and Urbich, 2018). In case of filament breakup, directly after collision a thin water bridge joins the two drops until it bursts into small fragments while the identities of the two colliding drops are substantially preserved. During sheet breakup, after collision a part of the larger drop forms an extending sheet of water from the impact area where the smaller drop often disappears. By disintegration of the sheet, a number of small fragments is formed. Thus, the smaller colliding drop is removed from the drop size spectrum whereas the larger drop basically preserves its identity. Disk breakup occurs when the two drops temporarily coalesce after collision and a water disk extends from the point of impact, incorporating the smaller drop. Finally, the disk gradually disintegrates producing a large number of small drops and eliminating the identities of the original colliding drop pair. Crown breakup represents a subset of disk breakup characterized by the formation of fewer and larger drops (all descriptions according to Testik et al., 2011). Similar to spontaneous breakup, collision-induced breakup is enhanced in an electric field that naturally occurs in deep convective clouds (Bhalwankar et al., 2023).

Experimental studies on the fragment size distribution of collision-induced breakup are rather limited so far as in laboratory experiments the proper realization and accurate measurement of atmospherically relevant parameters of colliding drops, such as drop and fragment sizes, terminal fall velocities, and impact angle are difficult. McTaggart-Cowan and List (1975) and Low and List (1982a) used an accelerator system designed for drop-drop collisions. Barros et al. (2008) conducted drop breakup experiments using a 14 m fall shaft to enable the interaction of two vertically falling drops. Emersic and Connolly (2011) employed an open wind tunnel to study collision-induced breakup, where one of the drops was levitated in a velocity dip in the center of the vertical air stream, another drop was injected from above – i.e., from downstream -, to collide with the stagnant drop. Similarly, Szakáll et al. (2014) performed experimental studies on drop-drop collisions in the Mainz vertical wind tunnel where the shape changes of raindrops during and after collision were analyzed.

The results of Low and List (1982a) still remain the major source for breakup parameterizations in numerical cloud models (Low and List, 1982b; McFarquhar, 2004) and serve as base for comparing new results (Schlottke et al., 2010; Szakáll et al., 2014). Schlottke et al. (2010) performed a numerical investigation of raindrop collisions; afterwards, the parameterization of Straub et al. (2010) includes their results together with the ones of Low and List (1982a). Later, Szakáll and Urbich (2018) compared the parameters obtained by Szakáll et al. (2014) to the parameterizations of McFarquhar (2004) and Straub et al. (2010). Although they found a good agreement between the parameterizations and the experimental results, there was an obvious difference for drop sizes smaller than the smallest colliding drop (i.e., less than 0.5 mm): fragments in that range are represented well by the McFarquhar (2004) parameterization but are missing in the Straub et al. (2010) size distribution.

An early parameterization was derived by Srivastana (1971) on the base of results from spontaneous breakup (Fournier d'Albe and Hidayetulla, 1955; Komabayasi et al., 1964), and the study of Blanchard and Spencer (1970) who observed drop breakup inside a fall shaft where it represents a mixture of spontaneous and collision-induced breakup. Thus, Srivastana (1971) claimed that the parameterization includes both processes.

In the present study, we combined model simulations with laboratory experiments. The laboratory experiments were performed at the Mainz vertical wind tunnel with freely floating drops under conditions close to that in real clouds. Spontaneous breakup of drops was investigated in both, laminar and turbulent flow to find out whether turbulence may enhance spontaneous breakup. Collision-induced breakup was conducted with a set of relevant drop sizes to determine important breakup parameters, in particular the fragment size distributions. The goal was to fill the gaps of missing drop sizes and to state if modification of earlier parameterizations is required. Besides that, process studies with a 3D cloud model were performed to define the most important breakup parameters that affect the cloud drop size distributions and precipitation. We tested the early parameterization of Srivastana (1971) and compared it to a new approach for collision-induced breakup based on the present results combined with results given by Low and List (1982a), Schlottke et al. (2010), and Szakáll and Urbich (2018).

2. Wind tunnel experiments

2.1. Methods: vertical wind tunnel

The experiments were performed at the Mainz vertical wind tunnel (Diehl et al., 2011) where cloud and raindrops can be investigated under conditions similar to that in the atmosphere. Two vacuum pumps maintain the continuous air flow through the tunnel. The air speed is controlled by a sonic valve which ensures precise as well as rapid variations. The tunnel has a uniform velocity distribution along the entire cross section area up to the boundary layer at their walls, which ensures that large drops are floating in a rather stable fashion for longer time periods in the observation section. Before entering the observation section, the air flow passes a honeycomb followed by a set of sieves, and is afterwards accelerated to a constant speed. Thus, the air stream in the observation section is laminar with a residual turbulence level below 0.5 %. An artificial turbulent flow can be generated by obstructing objects positioned upstream of the floating drop (Vohl et al., 1999; Vohl et al., 2001; Diehl et al., 2000; Jost et al., 2019). The observation section of the wind tunnel with a cross-sectional area of 17 × 17 cm^2 limits the experiments to the low wavelength range of the atmospheric turbulence spectrum, which is nonetheless relevant for cloud processes (Bodenschatz et al., 2010). During the experiments, the drops were recorded by a high-speed digital video camera (Motion ProX, Redlake, Inc.) mounted to the observation section of the tunnel. The camera captured images at a rate of 2000 fps (frames per second) with a resolution of 1280 × 1024 pixels and an image pixel size of 60 μm. Due to the size resolution of the camera setup the detectable fragment sizes were limited to 180 μm. Diffuse background illumination was used by a ground-glass plate in front of a 400 W DC cold light lamp. The drops were generated from distilled water. A scheme of the wind tunnel is shown in Fig. 1 that depicts the setup for the experiments with collision-induced breakup. For more details see Szakáll et al. (2010, 2014).

2.1.1. Spontaneous breakup

Individual drops with equivalent diameters between 8 and 13 mm were freely suspended at their terminal velocities under laminar and turbulent flow conditions. These two ambient conditions were applicated to determine whether turbulence, which is always present in and below clouds, has at all an impact on the survival of large raindrops. Previous studies indicated that cloud and precipitation processes are not

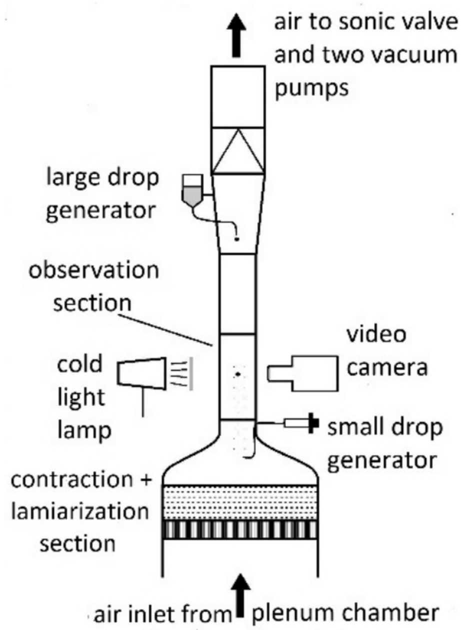

Fig. 1. Scheme of the Mainz vertical wind tunnel with the setup for collision-induced breakup experiments.

necessarily affected by ambient turbulence (e.g., Diehl et al., 2000; Vohl et al., 2001; Jost et al., 2019), allowing to neglect turbulence in numerical simulations of these processes. All together we observed about 300 drops in this set of experiments. It was a difficult task to control drops of these sizes as due to strong oscillations and eddy shedding (Szakáll et al., 2010) they perform sudden strong motions in all directions. This was even more the case under turbulent conditions and limited the numbers of observed drops as well as the observation times. The drops were injected by one person into the wind tunnel with two syringes and needles simultaneously to reach the desired drop sizes. They were manually controlled by another person by adapting the air speed accordingly. After releasing from the needles, the strong random motions and jumps had to be balanced sufficiently so that the drop did not get lost. In this way, suspending times of several minutes were achieved; however, in turbulent conditions this was less successful. The drop sizes were determined from the video recordings by using the same image analysis method as in Szakáll et al. (2014).

To induce turbulent flow conditions, we placed obstructing objects in the wind tunnel downstream of the observation section (see Fig. 1), a ring of 4 cm diameter as used before by Diehl et al. (2000) or a needle of 8 cm length as described by Vohl et al. (2001) and Jost et al. (2019). Both objects were tested to find the best method to successfully tackle the challenge to suspend the drops; however, in both cases suspending the drops was extremely difficult. Due to measurements with a hot wire instrument, the turbulent kinetic energy dissipation rate ε was between 0.1 $m^2\ s^{-3}$ and 0.5 $m^2\ s^{-3}$ for wind speeds around 8 m/s that were required to suspend the large drops.

2.1.2. Collision-induced breakup

Breakup after collision was studied with drop pairs of 4.0 to 5.2 mm and 1.9 to 3.1 mm in equivalent diameters. Our earlier experiments covered small drop sizes by investigating the collision between 2.5 mm and 0.5 mm drops (Szakáll et al., 2014). To decide which drop sizes should be investigated in the current experiments, we used the results of Testik (2009) who determined the ranges where drop collisions would affect breakup (in contrast to bounce or coalescence) in dependence on the Weber number and the drop size ratio $p = d_s/d_l$, with d_s the diameter of the small drop and d_l the diameter of the large drop. The dimensionless Weber number *We* (Pruppacher and Klett, 2010) describes the relative importance of the inertia forces to the surface tension:

$$We = \frac{\rho \frac{d_s}{2} (\Delta V)^2}{\sigma} \tag{1}$$

with ρ the density, σ the surface tension of water, and ΔV the relative speeds of the colliding drops: $\Delta V = \overrightarrow{V_1}$ - $\overrightarrow{V_2}$, where V_1 and V_2 are the velocities of the larger and the smaller of the colliding drops, respectively. Thus, we calculated *We* for different combinations of drop pairs to find out which combinations let expect breakup events.

During the experiments, individual drops of larger sizes were freely floated in the laminar air stream of the wind tunnel while drops of smaller sizes were introduced upstream of them, see Fig. 1. The challenge was to provide drop collisions in the observation section of the wind tunnel within the focus of the video camera. The larger drops came from a drop generator that was mounted at the upper part of the observation section. It consisted of a water supply in a pressure flask, which was joined to the wind tunnel by thin tubes ending in nozzles, from where drops entered the wind tunnel. The pressure in the flask (200 hPa above atmospheric pressure) controlled the water flow to the nozzles. To get drops of desired sizes, we selected the nozzle openings appropriately. Additionally, a wind speed of approximately 8.9 m/s was required to support the drops detaching from the nozzle. At the lower part of the observation section, the smaller drops were injected into the tunnel by a syringe and a long needle that was fixed at a wire cross in the center of the tunnel. The small disturbance in the cross center caused a small minimum of the air speed so that the drops were kept in balance (Jones and Saylor, 2009). The continuous generation of the larger drops from above together with the manual input of smaller drops from below allowed that drop collisions occurred in the observation section in front of the video camera. In case of drop collisions, the video camera was manually started to record the breakup type and the fragments after breakup. Finally, collisions of 137 drop pairs recorded by the video camera could be evaluated to determine parameters such as drop size, breakup efficiency and breakup type, and, in dependence on the breakup type, the number of fragments and the fragment size distributions after breakup.

2.2. Experiments: results and discussion

2.2.1. Spontaneous breakup

The drops in the laminar air stream, in particular the larger ones, showed extreme oscillations in horizontal mode that play a key role as supposed by Müller et al. (2013). We observed approximately 5 % spontaneous breakup events (8 breakup events of about 170 observed drops). In all these cases, the drop separated in the center forming two new drops of nearly equal sizes. Often it seemed as if the drop would breakup but then still remained together and came back to less oscillations. Such an example is given in Fig. 2. Because the drop motion during these experiments were rather strong in horizontal and vertical directions, it did not come about that a breakup event (which occurred anyhow rare) was recorded by the high-speed video camera, but we had the chance to record a video of a breakup event with a mobile phone.

The drops investigated in the turbulent air stream showed another oscillation behavior. The horizontal oscillation mode was not dominant but the drops were partly significantly deformed by several oscillation types mainly in vertical and transverse directions. We had the impression that this behavior promotes the coherence of the drops in contrast to the extreme oscillations in horizontal mode of the drops in the laminar air stream. The drops we observed did not undergo any breakup. Due to the challenge to freely float drops in a turbulent environment we were not able to observe them as long as the drops in the laminar air stream. Thus, one may argue that we missed breakup events as we lost the drops before. However, during their free suspension the drops did not show any tendency to break up, as the drops in the laminar environment did. Summarizing, our results confirm the findings of previous experimental

Fig. 2. Time sequence of drop floating in laminar air stream with extreme oscillations in horizontal mode. $\Delta t = 0.05$ s. From video recording with a mobile phone.

studies that drops larger than 8 mm in equivalent diameter may survive without breaking up (Pruppacher and Klett, 2010) but contradict the findings of Villermaux and Bossa (2009). However, as pointed out already in Szakáll et al. (2010), those experiments of Villermaux and Bossa (2009) were performed with a less appropriate measurement setup where breakup was probably artificially induced by the air jet due to its nonnatural strong small-scale wind shear.

2.2.2. Collision-induced breakup

Altogether, 137 colliding drop pairs were recorded, 61 collisions ended in coalescence, and 76 in breakup, giving a breakup efficiency of 0.55 for the investigated drop size range. Approximately half of breakup events resulted in two or three fragments. 40 collisions ended in the formation of more than 3 fragments, the maximum number of fragments was 9. Most of the breakup events (71) were filament breakup, while 5 events could be identified as disk breakup (according to Testik et al., 2011). Two examples of filament and disk breakup events are depicted in Fig. 3 as a time series.

In case of filament breakup (Fig. 3, left panel), the separated drop pair is visible at -13 ms, i.e. 13 ms before collision. After 3 ms, the two drops had collided directly and in a grazing fashion so that it seems as if the small drop had passed through the large drop. Afterwards, a water junction formed between the two drops that became thinner and finally, at 16 ms, disrupted into three small drops while the identity of the original drop pair had changed only a little. During disk breakup (Fig. 3, right panel), we note the drop pair at -5 ms before collision occurred at 0 ms. After 45 ms complete disintegration took place and the fragments were carried along with the air flow. The collision occurred near to the center of the large drop. The drops coalesced temporarily, but the disk that formed upon impact disintegrated into a large number of medium-sized drops. After breakup the original identities of the drops were lost.

The fragment size distributions formed after filament and disk breakup are given in Figs. 4 and 5 as columns. The size ranges were selected according to Straub et al. (2010); for each size range the numbers of fragments were determined from the video recordings. In Fig. 4, the results for filament breakup are summarized for two clusters of drop pairs, i.e. for several drop pairs with similar sizes, which represent the lower and the upper limits of the investigated size range. The comparison indicated that in both cases the sizes of the original drops, i.e. 4.0 and 1.9 mm as well as 5.5 and 2.9 mm, were part of the spectrum; however, in case of the smaller drop pairs, the sizes of the 4.0 mm drops were reduced to 3.5 mm after breakup. Additionally, we see the fragments that formed when the water bridge disrupted, which had smaller sizes than the original drops (i.e. smaller than 1.9 and 2.9 mm, respectively). In case of disk breakup, the results from all five disk breakup events were summarized for a cluster of drop pairs with equivalent diameters of 4.7 and 2.7 mm (Fig. 5). We note in comparison to Fig. 4 for filament breakup, that the spectral numbers of the larger fragments are significantly lower, reflecting that the original drops were eliminated by breakup, while the spectral numbers of the smaller fragments were higher, reflecting that more fragments formed by breakup.

For comparison, in both Figs. 4 and 5 fragment size distributions calculated with the parameterizations of McFarquhar (2004) and Straub et al. (2010) were included. The parameterization of McFarquhar (2004) distinguishes between filament and disk breakup while the one of Straub et al. (2010) does not. We note that McFarquhar (2004) describes the fragment size distributions for both breakup types qualitatively well, i.e. the fragment sizes are estimated well but the fragment numbers are partly overestimated. For disk breakup, Straub et al. (2010) describe the fragment numbers of sizes smaller than 1 mm and with sizes between 2

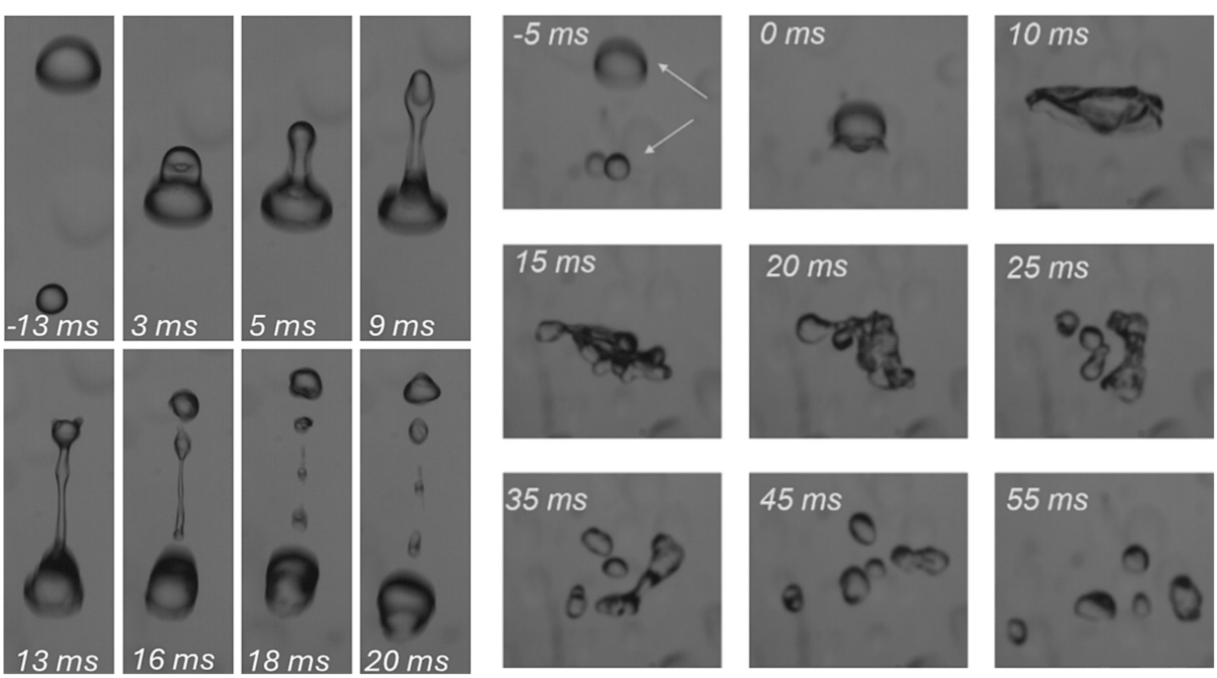

Fig. 3. Time series of breakup after collision of a large and a small drop. Left panel: filament breakup, equivalent drop diameters of 4.54 and 2.42 mm. Right panel: disk breakup, equivalent drop diameters of 4.56 and 2.56 mm.

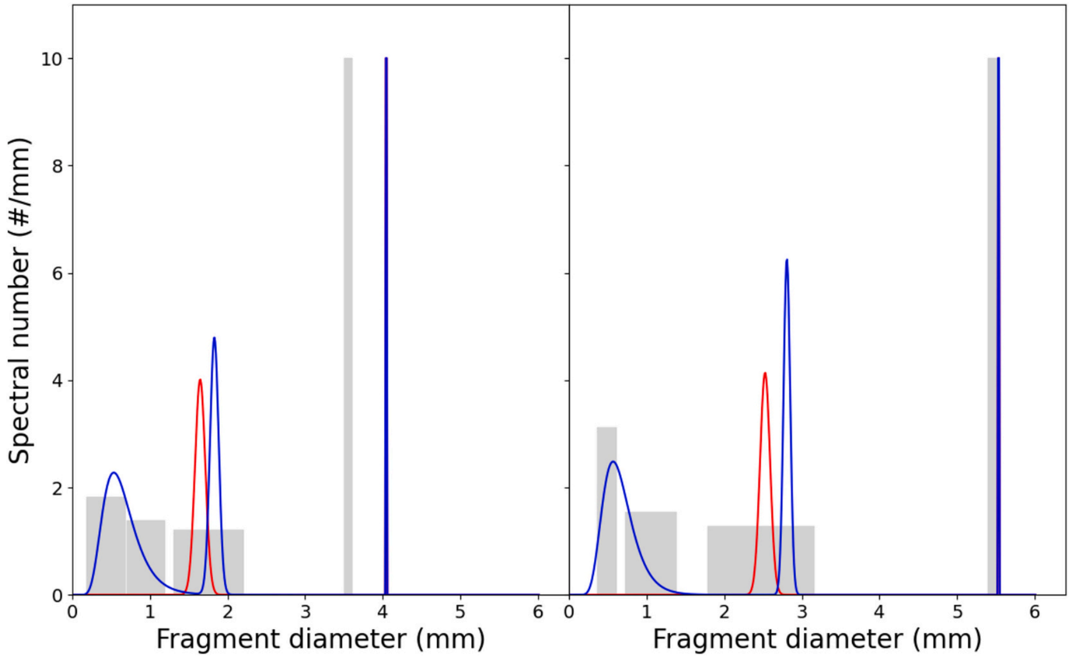

Fig. 4. Size distribution of fragments after filament breakup for two clusters of drop pairs with similar sizes. Fragment numbers between 2 and 3. Grey columns: present results from experiments. Average drop equivalent diameters, left panel: 4.0 and 1.9 mm, right panel: 5.5 and 2.9 mm. Blue and red lines: calculated according to the parameterizations of McFarquhar (2004) and Straub et al. (2010), respectively, for corresponding drop sizes. Spectral number: number per unit size interval. (For interpretation of the references to color in this figure legend, the reader is referred to the web version of this article.)

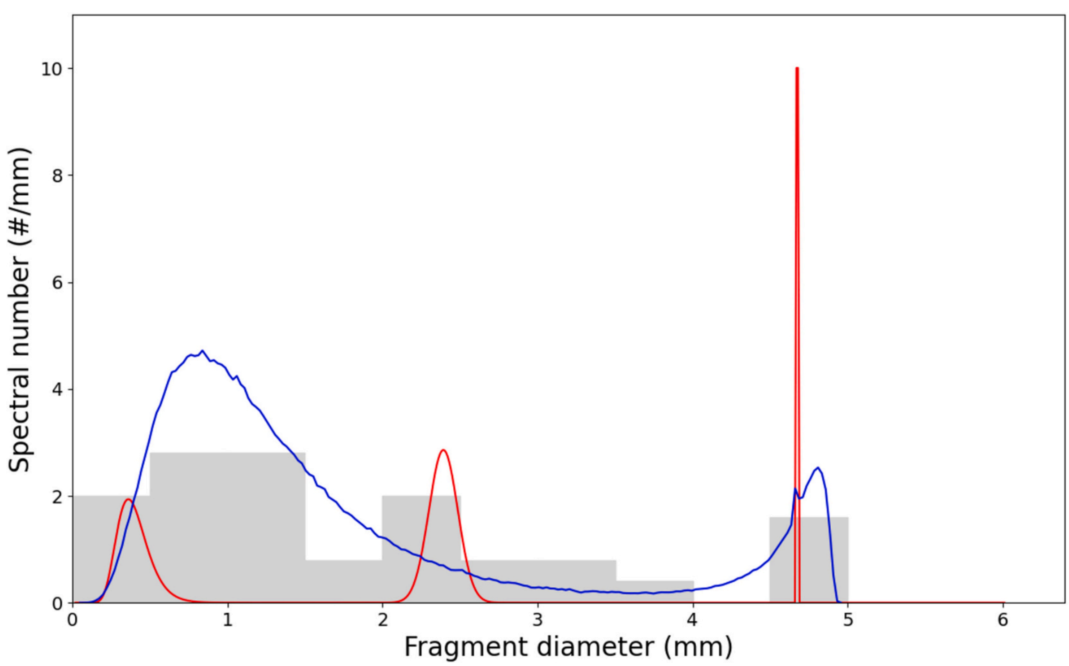

Fig. 5. Size distribution of fragments after disk breakup for a cluster of drop pairs with similar sizes. Fragment numbers between 5 and 9. Grey columns: present results from experiments, average drop equivalent diameters 4.7 and 2.7 mm. Blue and red line: calculated according to the parameterizations of McFarquhar (2004) and Straub et al. (2010), respectively, for corresponding drop sizes. Spectral number: number per unit size interval. (For interpretation of the references to color in this figure legend, the reader is referred to the web version of this article.)

and 3 mm well while the fragments in the 1 mm size range are missing and the numbers in the 4 to 5 mmm size range are overestimated (Fig. 5). In case of filament breakup (Fig. 4), it is obvious that the Straub et al. (2010) parameterization does not match with the experimental results and, thus, is not representative for this type of breakup. In case of disk breakup, the Straub et al. (2010) parameterization has to be modified.

Figure 6 shows the breakup efficiency as a function of the Weber number (Eq. 1) for the present and a number of previous experiments together with a fit to the data provided by Schlottke et al. (2010), which indicates that our new data match with the previous ones. The error bar of the data point derived from the present data resulted from the spread in the sizes of the drops released from the drop generators. The breakup efficiency exponentially increases with the Weber number *We*:

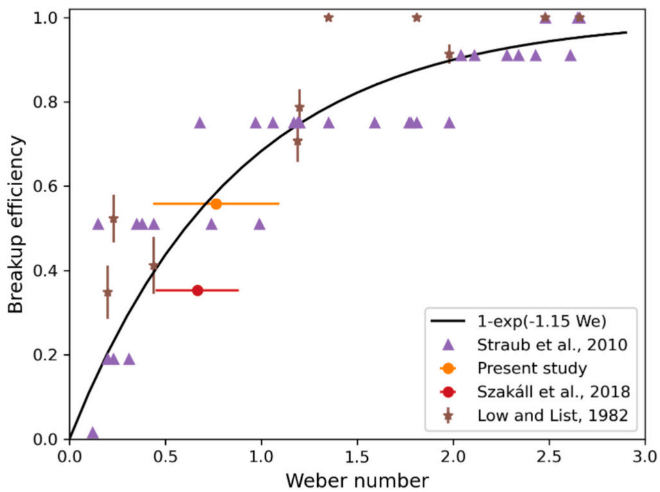

Fig. 6. Breakup efficiency as a function of Weber number. Data point from present study: from several measurements with error bar.

$$E_{break} = 1 - \exp(1 - 1.15\ We) \quad (2)$$

Thus, the larger the smaller colliding drop and the larger the difference between the two terminal velocities ΔV (the latter implying a larger difference between d_l and d_s), the more increases the breakup efficiency. This implies that breakup is more expectable for large Weber numbers because then the collision energy is larger than the surface energy that keeps the temporarily coalesced drop together. For small Weber numbers where the surface energy dominates the collision energy the collision results in coalescence of the two drops.

3. Process studies by implementing breakup parameterizations in a 3D cloud model

3.1. Methods: COSMO model

The model simulations were performed with the 3D cloud model COSMO-SPECS (Grützun et al., 2008; Diehl and Grützun, 2018), which contains a spectral bin-microphysics that explicitly solves the microphysical equations. The effect of breakup on the development of precipitation was studied by simulating convective clouds, which produce the largest raindrops (Pruppacher and Klett, 2010) so that breakup is potentially most important. Accordingly, convective vertical temperature and dew point profiles were used (Diehl and Grützun, 2018) to simulate an idealized convective cloud by a heat bubble over a flat terrain that was initialized by a temperature disturbance. It was located in the center of the domain (covering 80 × 80 × 18 km^3) at 1.4 km height with a horizontal extension of 5 km. We selected the temperature disturbance as 0.5 K, which resulted in a cloud reaching 11.5 km altitude after 45 min and dissipating afterwards by precipitation. The strongest vertical updraft in the cloud was noted after 30 min with vertical velocities up to 24 m/s in the cloud center.

The microphysical scheme (Diehl and Grützun, 2018) describes detailed cloud processes including entrainment. A fixed bin structure is used that combines wetted aerosol particles and liquid drops, divided into 66 size bins, starting with 0.002 μm in diameter, with a mass doubling in every category. After activating the initial dry aerosol particles (a mono-modal lognormal number size distribution from Kreidenweis et al., 2003), the particles and drops move in the spectrum by processes such as growth by water vapor deposition, shrinking by evaporation, collision and coalescence of drops, and impaction scavenging of particles. Detailed freezing processes are also included in the scheme but were turned off during the present investigations. A new parameterization based on recent and present experiments of collision-induced breakup was derived and compared to an earlier one based on experiments of mixed spontaneous and collision-induced breakup (Srivastana, 1971).

3.1.1. Parameterization according to Srivastana (Sriva)

Srivastana (1971) derived a parameterization on the base of experimental studies including spontaneous as well as collision-induced breakup. Drops reaching a critical size may breakup according to a probability function P in s^{-1} and generate drops with a defined size distribution Q. In the microphysical scheme, variable parameters were the starting size bin J_{start} and the smallest target size bin after breakup J_{tar}. All drops in size bins $J \geq J_{start}$ had the chance to breakup according to the probability P, which increases with the size bin J. After breakup, the available water mass was distributed in the bins between J_{tar} and J and the number of fragments was calculated according to the size distribution Q for each of these bins. For details see Srivastana (1971). We performed sensitivity studies where we selected bins 58, 60, and 62 as J_{start} (corresponding to drop diameters of 1200, 1905, and 3024 μm, respectively) and size bins between 47 and 54 as J_{tar} (corresponding to drop sizes from 95 to 476 μm). This description was incorporated into the microphysical scheme so that all drops with corresponding sizes had the chance to breakup. The list of the simulated cases is given in Section 3.2.1.

3.1.2. New parameterization of collision-induced breakup (Coll)

In the microphysical scheme, the collisions of drops are described by the linear discrete method (Simmel and Wurzler, 2006) including the collision kernel of Kerkweg et al. (2003) and the corresponding terminal velocities for each colliding drop pair. In previous studies, colliding drop pairs were assumed to coalesce with an efficiency of 1 (Diehl and Grützun, 2018). In the present study, not all colliding drops were allowed to remain together. In the model routine where drop collisions are described, collision-induced breakup was calculated after the drop collision loop in each time step, based on previous (Low and List, 1982a; Schlottke et al., 2010; Szakáll and Urbich, 2018) and present results. For potential breakup we considered the sizes of the resulting drops after an assumed coalescence. The sizes of drops – after hypothetical coalescence – that were observed to break up had sizes of 1200 μm in diameter or larger, which corresponds to size bin 58 in the microphysical scheme. Based on the literature given above, for each size bin between 58 and 65 the parameters breakup efficiency E_{break} and number of fragments N_{frag} were compiled. From the ranges of the data, mean values were estimated for each size bin considering the frequency of occurrence, as listed in Table 1.

The breakup efficiency E_{break} ranged from 0.2 to 0.9; taking into account the mean values we varied E_{break} between 0.4 and 0.75 in the sensitivity studies and selected 0.65 as a realistic value for all size bins (considering Fig. 6). The mean numbers of fragments N_{frag} ranged from 2 to 14; we varied them between 2 and 16 and selected values from 2 to 8 as realistic ones, in dependence of the drop size. Note that breakup into two drops means that the drop number remains the same but the drop sizes may be different after collision. This is not the same as bounce where the two colliding drops just touch and keep their identity. The list of the simulated cases is given in Section 3.2.1.

To estimate the effects of the fragment sizes on the development of cloud microphysics and precipitation, several approaches were selected. On one hand, drops of equal sizes were formed after breakup while on the other hand a drop size spectrum was generated. The sizes and numbers of the drops after breakup had to match in a way that the sums of masses and volumes of these drops agree with mass and volume of the breaking drops (mass and volume conservation). In Table 2, the drop numbers after breakup and the size bins into which the drops were sorted are listed. K was the size bin before breakup, i.e. any size bin larger than 58 (the smallest size bin where breakup was allowed). When equally sized drops formed after breakup, then the target bins for breakup were (K-1) for breakup into 2 drops, (K-2) for breakup into 4 drops, (K-3) for breakup into 8 drops, and (K-4) for breakup into 16

Table 1
Values of breakup efficiencies and fragment numbers as derived from the literature: Low and List, 1982a (LL1982); Schlottke et al., 2010 (SC2010); Szakáll and Urbich, 2018 (SU2018); present study (PS2025) with mean values. Model range: values used in the sensitivity studies. Model realistic values: based on mean values from literature. Size bins and diameters after hypothetical coalescence.

size bin	mean diameter µm	reference	E_{break} from literature	E_{break} mean values fr. literature	N_{frag} from literature	N_{frag} mean values fr. literature	E_{break} model range	E_{break} model realistic value	N_{frag} model range	N_{frag} model realistic value
58	1200	SC2010	0.5–0.75	0.625	2	2	0.4–0.7	0.65	2–4	2 / 4
59	1512	SC2010	–	–	–	–	0.4–0.7	0.65	2–4	2 / 4
60	1950	SC2010	0.5–0.75	0.625	2	2	0.4–0.7	0.65	2–16	2 / 4
61	2400	SC2010	0.75	0.75	2	2	0.4–0.7	0.65	2–16	2 / 4
62	3024	SC2010 SU2018	0.4–0.9	0.73	2–8	3.25	0.4–0.75	0.65	4–16	4
63	3810	LL1982 SC2010 PS2025	0.2–0.9	0.65	2–14	5.2	0.4–0.75	0.65	4–16	4 / 5 / 7
64	4800	LL1982 SC2010 PS2025	0.2–0.9	0.62	2–14	7.5	0.4–0.75	0.65	4–16	5 / 7 / 8
65	6048	PS2025	–	0.55	2–9	4.6	0.4–0.75	0.65	4–16	5 / 7 / 8
66	7622	–	–	–	–	–	0.4–0.75	0.65	4–16	5 / 7 / 8

Table 2
Fragment numbers after breakup and size bins into which the new drops were sorted. K is the size of the drop before breakup.

N_{frag}	drops after breakup	K-1	K-2	K-3	K-4	K-5	K-6	K-7	K-8	K-9	K-10	K-11	K-12	breakup type
2	equal sizes	2	–											filament
4	equal sizes	–	4	–										disk
8	equal sizes	–	–	8	–									disk
16	equal sizes	–	–	–	16	–								disk
4	spectrum 1a	1	1	2	–	–								filament
8	spectrum 1b	–	2	2	4	–								disk
7	spectrum 2	1	2	–	–	–	–	–	–	–	–	1	3	filament
5	spectrum 3	1	2	–	–	–	–	–	–	1	–	1	–	filament

drops. This sorting is a consequence of the mass doubling in every size bin. In cases where the drops formed a spectrum after breakup, we selected the target size bins accordingly. With spectrum 1, larger and smaller drops were formed simultaneously, the spectrum covered three size bins. Spectrum 2 covered twelve size bins and contained rather large drops together with small drops. Spectrum 3 covered 10 size bins and contained large, moderate sized, and small drops.

The fragment size distributions after breakup reflect the breakup types. When the fragment size distribution contained drops in the size bin (K-1), this case can be considered as filament breakup where the water junction between the colliding drops disrupted into small drops while larger drops remained from the two original ones. The other cases

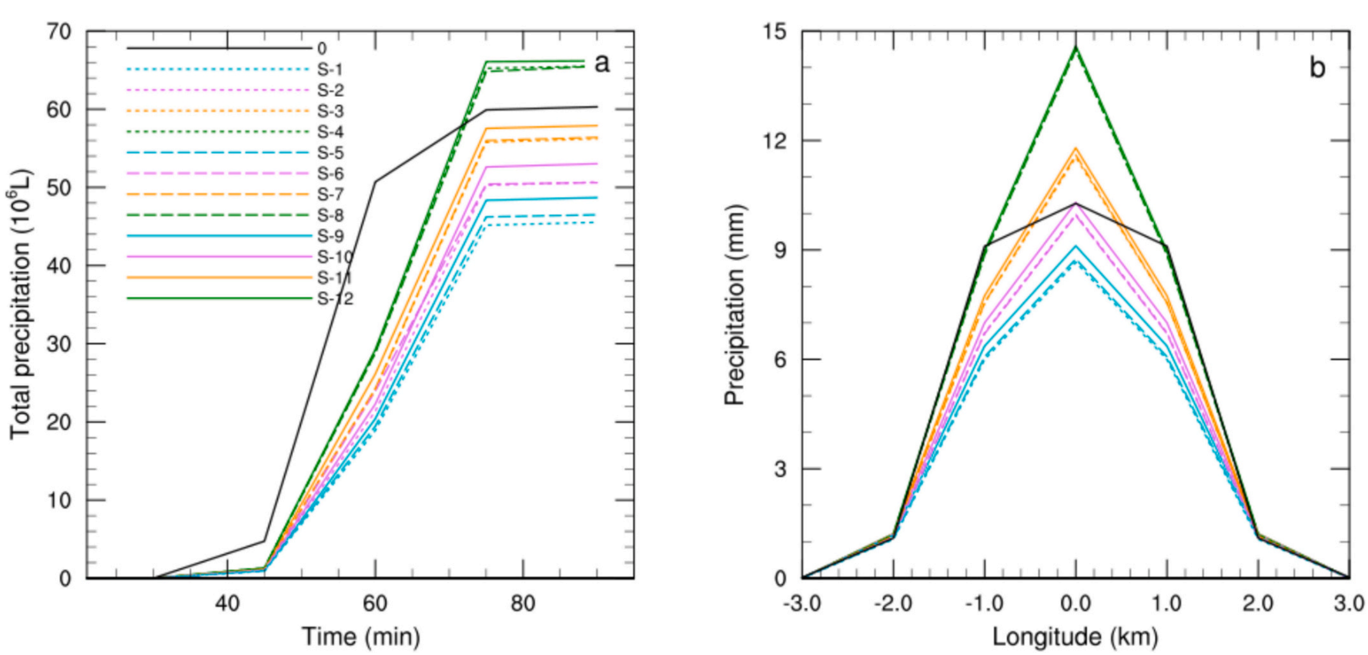

Fig. 7. (a) Temporal development of precipitation during 90 min modeling time for the Sriva cases. (b) Local distribution of precipitation through the cloud after 90 min. Cases as listed in Table 3; same color means same value of J_{tar}, dotted lines: d_{start} = 1200 µm, broken lines: d_{start} = 1905 µm, solid lines: d_{start} = 3024 µm.

can be considered as disk breakup where the original drop pair is eliminated and larger numbers of new drops are formed (see Section 2.2.2).

3.2. Process studies with breakup parameterizations: Results and Discussion

3.2.1. Results from breakup according to Srivastana (Sriva)

Precipitation results from the Sriva cases are summarized in Fig. 7 and listed in Table 3. It was found that precipitation formation is dependent on both parameters J_{start} and J_{tar} but much more sensitive to J_{tar}. The smaller the drop sizes after breakup, the higher reduction of precipitation was found in comparison to case 0 without breakup. With larger size bins J_{tar}, precipitation was nearly equal for different starting bins J_{start} (e.g., cases S-4, S-8, and S-12 with $d_{break,\min} = 476$ μm), but the results differed more and more with decreasing J_{tar} (e.g., cases S-1, S-5, and S-9 with $d_{break,min} = 95$ μm). From Fig. 7 it is obvious, that breakup affected a delay of precipitation in the way that the amount after 45 min was reduced as well as the increase at later times, even when the total amount was similar or even higher than in case 0. Looking at the local distribution of precipitation, we note from Fig. 7b that it was more concentrated in the center of the cloud area in all Sriva cases and more evenly distributed in case 0.

Comparing the drop spectra for case 0 without breakup and the Sriva cases S-1 and S-3 (Fig. 8), we observe significant differences over the entire range of drop sizes. In case 0, the drop size spectra contained high numbers of small diameters (< 60 μm) at high altitudes and low numbers of large drops ranging from 2 to 10 mm that were reaching the ground as precipitation. The Sriva cases showed less drops at high altitudes as case 0 but more drops near the ground, many of them with sizes between 60 and 600 μm and small numbers with sizes around 3 mm. Precipitation was lower in Sriva cases S-1 and S-3 (45×10^6 L and 56×10^6 L) as in case 0. Drops larger than 4 mm were reduced in comparison to case 0 due to breakup. In particular, precipitation was dominated by drops ranging from 50 to 300 μm in case S-1, and from 200 to 400 μm in case S-3. This is according to the lower J_{tar} value in case S-1. Note in this context that the drop volume significantly increases with increasing size. For instance, a 6 mm drop has a volume of approximately 1.1×10^{-4} L, in contrast to 4.2×10^{-9} L of a 200 μm drop.

3.2.2. Results from collision-induced breakup (Coll)

Precipitation results from the Coll cases are given in Table 4 and in Fig. 9. Breakup was allowed for all size bins $J \geq J_{start}$. In a first set of model simulations, we chose one value of N_{frag} and E_{break} for all size bins larger than the threshold value J_{start} (cases C-1 to C-10). In a second set, we used combinations of one to three values of N_{frag} and E_{break} in dependence on the drop sizes. The combination of the parameters J_{start} and N_{frag} implied the smallest drop sizes as a result of breakup. In cases C-1 to C-13, the drop fragments had equal sizes after breakup, while in cases C-14 to C-16 we simulated the formation of a drop size spectrum after breakup as described in Section 3.1.2.

Table 3
Precipitation results from simulated cases with the Srivastana (1971) breakup parameterization; values in bold type: reduced precipitation in comparison to case 0. d_{start} is the corresponding drop diameter to size bin J_{start}, d_{break} gives the size range of the new drops after breakup ranging from the size bins J_{tar} and J.

case no.	J_{start}	J_{tar}	d_{start} (μm)	d_{break} (μm)	total precipitation ($\times 10^6$ L)
S-0	–	–	–	–	60
S-1	58	47	1200	95–6048	**45**
S-2	58	50	1200	190–6048	**51**
S-3	58	52	1200	300–6048	**56**
S-4	58	54	1200	476–6048	66
S-5	60	47	1905	95–6048	**46**
S-6	60	50	1905	190–6048	**51**
S-7	60	52	1905	300–6048	**56**
S-8	60	54	1905	476–6048	66
S-9	62	47	3024	95–6048	**49**
S-10	62	50	3024	190–6048	**53**
S-11	62	52	3024	300–6048	**58**
S-12	62	54	3024	476–6048	66

Fig. 9a shows precipitation results from the first set of model simulations with fixed values of N_{frag} or E_{break} (i.e. cases C-1 to C-10). They indicate that with $N_{frag} = 4$, the total amount of precipitation decreased when increasing E_{break} from 0.4 to 0.75 (cases C-1 to C-6). In comparison to case 0 without breakup, precipitation was higher or equal in cases C-1 to C-4 but lower in cases C-5 and C-6 with a breakup efficiency $E_{break} \geq 0.7$. With $N_{frag} = 8$ (cases C-7, C-9, and C-10), precipitation was significantly lower than case 0 when $E_{break} \geq 0.65$. In cases C-2 and C-4, two parameters were kept fixed and J_{start} was enhanced from 58 to 62, which resulted in slightly decreased precipitation. With fix $E_{break} = 0.6$, precipitation significantly decreased when increasing N_{frag} from 8 to 16 (cases C-7 and C-8). In case C-7, the precipitation amount was similar as in case 0 without breakup but it was lower in case C-8 with $N_{frag} = 16$. Thus, the following settings considerably reduce precipitation: $N_{frag} = 4$ together with $E_{break} \geq 0.7$, $N_{frag} = 8$ together with $E_{break} \geq 0.65$, $N_{frag} > 8$. In accordance with these results, cases C-11 to C-13 with combinations of two or three N_{frag} values resulted in less precipitation than case 0 (Fig. 9c), in particular case C-12 with a breakup efficiency $E_{break} = 0.7$.

Cases C-14 to C-16 in which we simulated the formation of a drop size spectrum after breakup affected similar precipitation amounts as in the corresponding cases with the formation of equal drops (cases C-14 vs C-13, C-15 vs. C-11, C-16 vs. C-3; the comparing cases were selected according to the numbers of fragments). We note from Fig. 9c that the courses of the corresponding cases were similar. With spectrum 1 (C-14) and 2 (C-15), precipitation was slightly enhanced in comparison to the corresponding cases but it was reduced with spectrum 3 (C-16). However, in general the resulting precipitation amounts did not differ significantly from each other. In comparison to case 0 without breakup, precipitation was slightly reduced. Nevertheless, precipitation was delayed by 15 min in the breakup cases (Figs. 9a and c) when compared to case 0 but it increased fast afterwards in cases where the precipitation amount was similar as in case 0 (cases C-1, C-2, C-3, C-7, C-11, C-15, C-16). Precipitation was more concentrated in the center of the cloud area (Figs. 9b and d) except in cases C-15 and C-16 where drop spectrum 2 or 3 was formed after breakup that cover a broader spectrum of drop sizes (see Table 2). There we found more rain from the edges of the cloud similar as in case 0.

Figure 10 shows the drop spectra after 45 min for selected Coll cases. Differences are visible in the size range above 60 μm diameter, in particular above 600 μm diameter. For cases with the formation of a drop spectrum after breakup and the corresponding cases where equal sized drops were formed, the drop size spectra were rather similar (cases C-14 vs. C-13, C-15 vs. C-11, C-16 vs. C3) while between the case pairs we noted some differences. Thus, it seems that the number of fragments has more effects on the drop size spectrum than the specification whether the drop fragments have equal or different sizes. In comparison to case 0 without breakup (see Fig. 8), the drop sizes were reduced, mostly in cases C-11, C-13, and C-14, so that more drops in the size range around 3 mm were present. However, drops near ground as precipitation had diameters from 2 to 8 mm, similar as in case 0 (maximal sizes 10 mm).

3.2.3. Process studies with breakup parameterizations: Discussion

Comparing the drop size spectra of the Coll cases to the Sriva cases (Figs. 8 and 10), we note that the differences between case 0 and the Coll cases on one hand and the Sriva cases on the other hand were significant. Precipitation in the Sriva cases was dominated by much smaller drops, i.e. with diameters from 200 to 400 μm in case S-3 that resulted in a similar precipitation amount as the Coll cases shown in Fig. 10. This is directly implied by the Sriva parameterization in which more drops are formed in smaller size bins (compare Fig. 1 in Srivastana, 1971). In

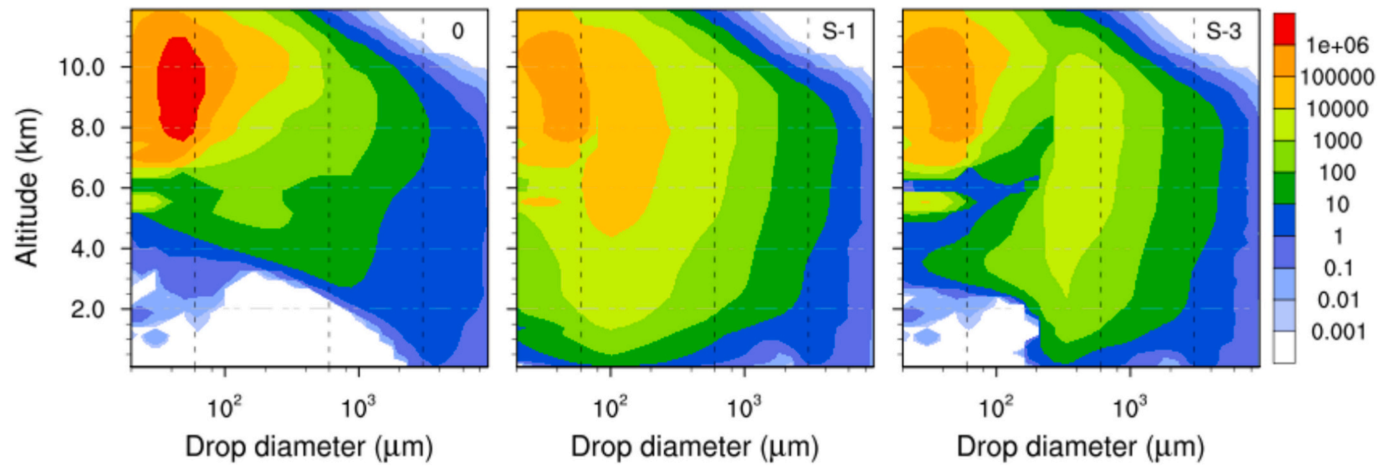

Fig. 8. Drop size spectra at 45 min in the center cell of the cloud for case 0 without breakup and two Sriva cases (1 and 3) according to Table 3. Number concentrations (color scale) in m^{-3}, vertical lines: 60 µm, 600 µm, and 3 mm drop diameter.

Table 4
Precipitation results from simulated cases with collisional breakup of drops; values in bold type: reduced precipitation in comparison to case 0. d_{break} gives the size range covered by the new drops after breakup.

case no.	J_{start}	d_{start} (µm)	J_{break}	d_{break} (µm)	E_{break}	N_{frag}	drops after breakup	total precipitation ($\times 10^6$ L)
0	–	–	–	–	–	–	–	60.3
C-1	58	1200	56–64	756–4800	0.4	4	equal sizes	63.7
C-2	58	1200	56–64	756–4800	0.6	4	equal sizes	63.0
C-3	58	1200	56–64	756–4800	0.65	4	equal sizes	62.5
C-4	62	3024	60–64	1905–4800	0.6	4	equal sizes	60.6
C-5	62	3024	60–64	1905–4800	0.7	4	equal sizes	**52.8**
C-6	62	3025	60–64	1905–4800	0.75	4	equal sizes	**48.4**
C-7	60	1905	57–63	953–3811	0.6	8	equal sizes	60.3
C-8	60	1905	56–62	756–3024	0.6	16	equal sizes	**45.2**
C-9	63	3811	60–63	1905–3811	0.65	8	equal sizes	**44.0**
C-10	63	3811	60–63	1905–3811	0.75	8	equal sizes	**34.9**
C-11	58	1200	56–64	765–4800	0.65	4	equal sizes	**56.3**
	63	3024	59–63	1512–3811		8		
C-12	62	3024	60–64	1905–4800	0.7	4	equal sizes	**39.0**
	64	4800	61–63	2400–3811		8		
C-13	58	1200	57–60	953–1905		2		**54.3**
	62	3024	60–61	1905–2400	0.65	4	equal sizes	
	64	4800	61–63	2400–3811		8		
C-14	58	1200	57–60	953–1905		2	equal sizes	**56.7**
	62	3024	59–62	1512–3024	0.65	4	spectrum 1	
	64	4800	60–64	1905–4800		8	spectrum 1	
C-15	58	1200	56–60	756–1905	0.65	4	equal sizes	**57.8**
	63	3811	51–65	238–6048		7	spectrum 2	
C-16	58	1200	56–60	756–1905	0.65	4	equal sizes	**59.2**
	63	3811	51–65	300–6048		5	spectrum 3	

contrast, the Coll parametrization distributes the drops after breakup more singularly to the size classes, which represents a situation closer to the real case as demonstrated in recent and the present experimental studies.

Precipitation was delayed by breakup due to smaller drop sizes after breakup, as was expected because more time is needed during cloud evolution to form precipitation-sized drops. In most cases, it was found that precipitation was more concentrated in the cloud center. Exceptions were the cases where a broad drop spectrum was formed, containing small, moderate sized, and large drops, representing filament breakup. Here the local distribution of precipitation was more evenly distributed similarly as in case 0. The total precipitation amount could be significantly reduced when small drops were formed (Sriva cases) or when the breakup efficiency and the fragment numbers were high (Coll cases).

To contextualize the cases from our sensitivity studies in view of the real cloud situation, we may consider the smallest drop diameters after breakup. According to previous studies these were 250 to 500 µm (Schlottke et al., 2010), 200 µm (Szakáll and Urbich, 2018), and 240 µm found in the wind tunnel experiments of the present study. However, these values do not necessarily represent the real smallest drop sizes after breakup but may be limited by the measurement resolution. Thus, cases with realistic settings for Sriva parameterizations were those, where the smallest drops after breakup had diameters of 300 µm or less (see Table 3), and Coll cases C-15 and C-16 with the smallest drop diameters of 238 and 300 µm. Considering breakup efficiencies and fragment numbers, Coll cases C-11, C-13, and C-14 could be assumed as realistic cases, too. In all these cases, the total amount of precipitation was reduced but not significantly. This may, however, be valid only for the investigated case of a convective cloud and may change, e.g., in a deep convective cloud system with even higher numbers of large drops. However, in such cases ice formation has to be considered as well while the present sensitivity studies focused on the warm rain formation.

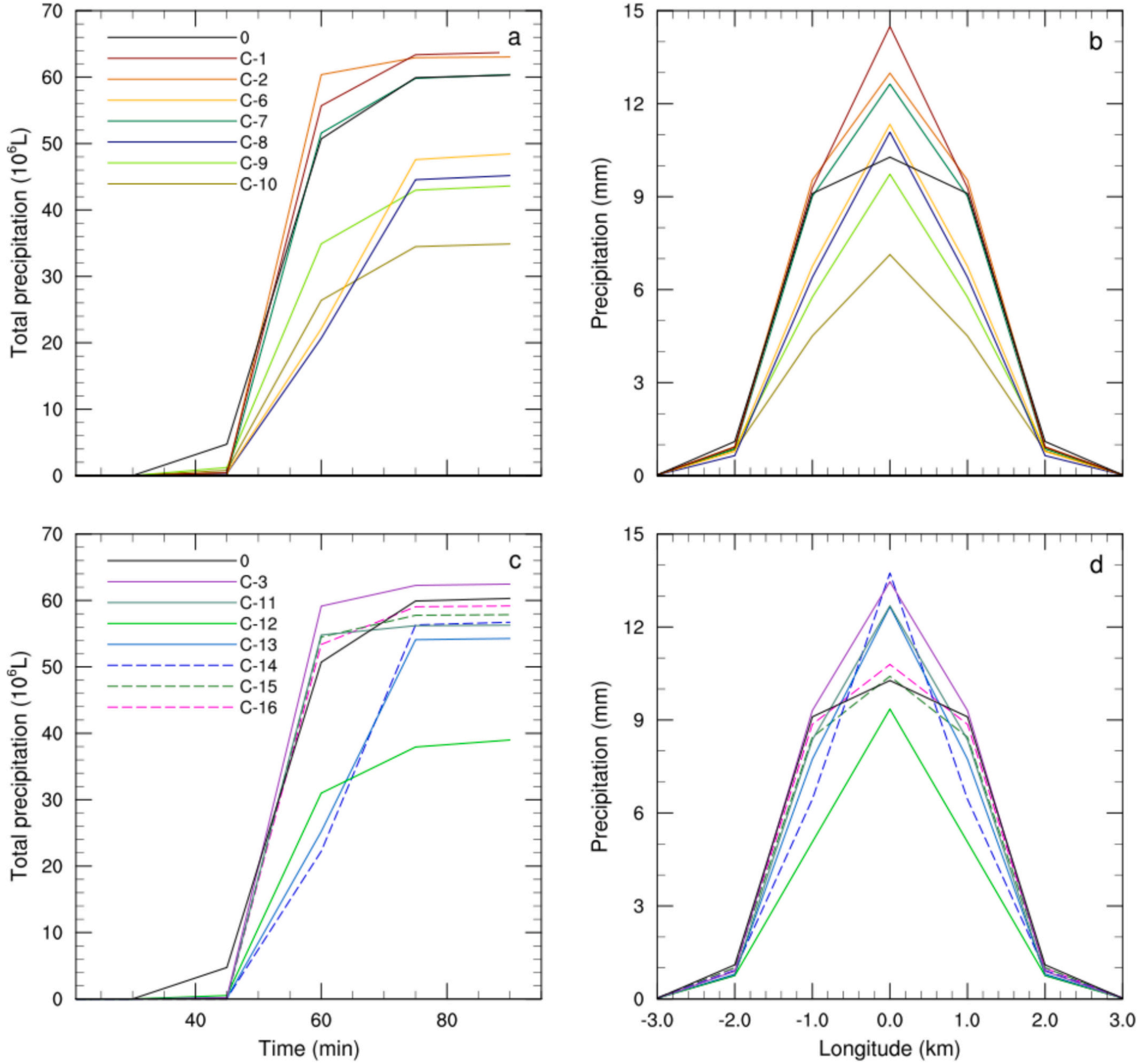

Fig. 9. (a) and (c) Temporal development of precipitation during 90 min modeling time, (b) and (d) local distribution of precipitation through the cloud after 90 min, for selected cases as listed in Table 4. Solid lines: equal sized drops after breakup, broken lines: drop spectrum after breakup. Similar colors show corresponding cases.

4. Summary and conclusions

Two types of drop breakup were investigated in the Mainz vertical wind tunnel with freely floating drops under conditions close to that in real clouds. Spontaneous breakup occurs when the energy of the natural drop oscillation exceeds the surface energy; it was studied in a laminar and a turbulent environment. The experiments showed that the increasing amplitude of the horizontal oscillation mode with increasing size plays a key role. Under laminar conditions, about 5 % of the observed drops with equivalent diameters between 8 and 13 mm broke up. In all cases, the drop separated in the center and formed two new drops of equal sizes. Turbulences in the airflow changed the drop oscillation in the way that several oscillation types mainly in vertical and transverse directions caused significant deformations of the drops. However, this behavior seemed to promote the maintenance of the drops in contrast to the extreme oscillations in horizontal mode of the drops in the laminar air stream. Thus, we conclude that spontaneous breakup plays, if at all, a minor role and may be neglected in cloud models. Our observations validated that drops larger than 6 mm in diameter are able to survive without spontaneous breakup, which contradicts the findings of Villermaux and Bossa (2009). As pointed out already in Szakáll et al. (2010), their measurement setup might be inappropriate so that breakup was probably artificially induced by the air jet due to its nonnatural strong small-scale wind shear.

Thus, breakup is more likely to occur during drop collisions where they may break up into several fragments. Our experiments with collision-induced breakup indicated a breakup efficiency of 0.55 for the investigated drop pairs with mean diameters of 4.6 and 2.5 mm. The numbers of fragments ranged from 2 to maximal 9, but approximately half of breakup events resulted in 2 or 3 fragments. The most frequent breakup type was filament breakup, which agrees with the findings of Testik et al. (2011). Regarding the collisional breakup efficiency as a

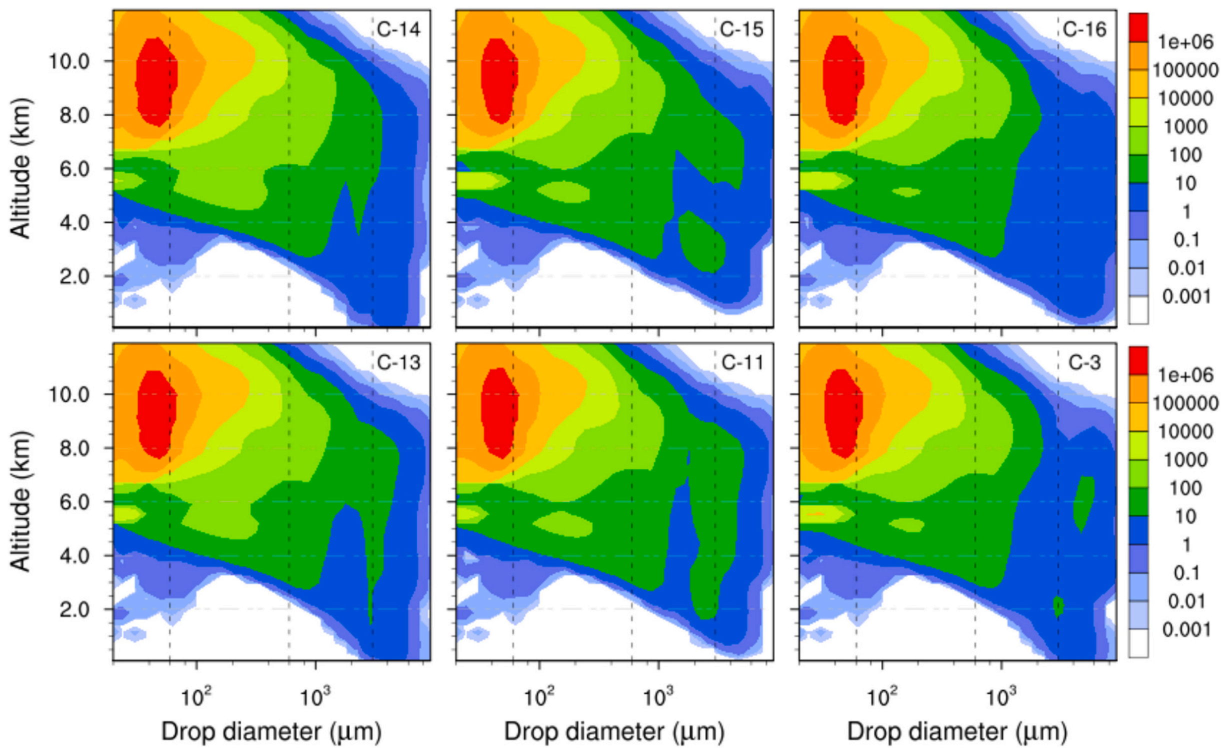

Fig. 10. Drop size spectra at 45 min in the center cell of the cloud for selected Coll cases according to Table 4. Number concentrations (color scale) in m^{-3}, vertical lines: 60 µm, 600 µm, and 3 mm drop diameter. Upper line: cases with formation of drop spectrum after breakup, lower line: corresponding cases with formation of equal sized drops.

function of the Weber number, the comparison of our present and a number of previous experiments indicates that our new data match with the previous ones. The breakup efficiency exponentially increases with the Weber number so that breakup is more expectable for large Weber numbers because then the collision energy is higher than the surface energy that keeps the drop together.

The comparison of our measured fragment size distributions to those given by two recent parameterizations indicated that the Straub et al. (2010) parameterization is not suited to describe the fragment size distribution after filament breakup. For disk breakup, it has to be modified in the way that the formation of fragments in the 1 mm and in the 4 5o 5 mm size ranges is reproduced. In contrast, we found that the parametrization of McFarquhar (2004), which distinguishes between filament and disk breakup, describes the fragment size distributions qualitatively well, even when including the present results for colliding drop pairs of larger sizes. Some modifications regarding the fragment numbers would improve the parameterization.

Numerical simulations were performed where a new parameterization of collision-induced breakup was compared to the early parameterization of Srivastana (1971). The latter was derived from early measurements and includes a breakup probability that increases with drop size and a size distribution of the fragments, which results in increasing numbers with fragment size. The parameter giving the smallest drop size after breakup determines the cloud drop size distribution and, thus, the total amount of precipitation. However, with the knowledge of more recent experimental results, the Srivastana parameterization might not adequately represent the drop spectrum after breakup. If it is used in cloud models, we would recommend to set the values of the parameters J_{start} and J_{tar} such that breakup starts with drops of 1200 µm diameter and that the smallest drops after breakup have diameters of 300 µm or less, due to the findings from previous literature (Low and List, 1982a; Schlottke et al., 2010; Szakáll and Urbich, 2018) and the present study.

The new parameterization of collision-induced breakup is based on more recent literature (Low and List, 1982a; Schlottke et al., 2010; Szakáll and Urbich, 2018) and this study. Thus, it considers mainly the same data as the parameterizations of McFarquhar (2004) and Straub et al. (2010) but complemented in the range of larger drops by results from Szakáll and Urbich (2018) and the present study. However, in contrast to those parameterizations, it is coupled with the existing drop collision description of the microphysical bin scheme. Important parameters are the breakup efficiency and the number of fragments after breakup. In particular the latter seems to have more effects on the cloud drop size spectrum than the specification whether the drop fragments have equal or different sizes. Thus, the type of the drop spectrum after breakup – and, implicitly, the type of breakup – may to have only secondary effects on the drop size distribution and, thus, on precipitation amounts. Nevertheless, the formation of a drop spectrum containing drops of large, moderate, and small sizes comes closest to the experimentally determined drop spectra. The present parameterization is applicable in cloud models containing a spectral bin-microphysics with an appropriate description of drop collisions. Then the drops formed by collision can be divided in coalescing fractions and breakup fractions and the breakup conditions, i.e. breakup efficiency and numbers and sizes of fragments, can be provided as look-up tables in dependence of the drop sizes.

Similar as Seifert et al. (2005), we found that breakup reduces the numbers of large raindrops and delays the onset of precipitation. Additionally, it may change the local distribution in the way that precipitation is more concentrated in the cloud center. Finally, it can reduce the total precipitation amounts but not significantly under conditions close to the real case. This may, however, be valid only for the investigated case of a convective cloud and may change, e.g., in a deep convective cloud system with even higher numbers of large drops. However, in such cases ice formation has to be considered as well while the present sensitivity studies focused on the warm rain formation.

CRediT authorship contribution statement

Karoline Diehl: Writing – original draft, Software, Methodology, Conceptualization. **Tobias Jungbluth:** Investigation, Formal analysis. **Alexander Theis:** Writing – review & editing, Methodology. **Subir K. Mitra:** Methodology. **Miklós Szakáll:** Writing – review & editing, Supervision, Software, Methodology, Funding acquisition, Conceptualization.

Declaration of competing interest

The authors declare that they have no known competing financial interests or personal relationships that could have appeared to influence the work reported in this paper.

Acknowledgements

This work was funded by the Deutsche Forschungsgemeinschaft (DFG, German Research Foundation) – 431120337. The model simulations were performed at the High-Performance Cluster MOGON II at the University of Mainz. The authors thank Axel Seifert for fruitful discussions and support.

Data availability

Data will be made available on request.

References

Barros, A.P., Prat, O.P., Shrestha, P., Testik, F.Y., Bliven, L.F., 2008. Revisiting Low and List (1982): Evaluation of raindrop collision parameterizations using laboratory observations and modeling. J. Atmos. Sci. 65 (9), 2983–2993.

Bhalwankar, R.V., Pawar, V., Kamra, A.K., 2023. Binary collisions of water drops in presence of horizontal electric fields: a wind tunnel study. J. Geophys. Res. 128. https://doi.org/10.1029/2022JD037543 e2022JD037543.

Blanchard, D.C., Spencer, A.T., 1970. Experiments on the generation of raindrop-size distributions by drop breakup. J. Atmos. Sci. 27, 101–108.

Bodenschatz, E., Malinowski, S.P., Shaw, R.A., Stratmann, F., 2010. Can we understand clouds without turbulence? Science 327, 970–971.

Diehl, K., Grützun, V., 2018. Model simulations with COSMO-SPECS: impact of heterogeneous freezing modes and ice nucleating particle types on ice formation and precipitation in a deep convective cloud. Atmos. Chem. Phys. 18, 1–21.

Diehl, K., Vohl, O., Mitra, S.K., Pruppacher, H.R., 2000. A laboratory and theoretical study on the uptake of sulfur dioxide gas by small water drops containing hydrogen peroxide under laminar and turbulent conditions. Atmos. Environ. 34, 2865–2871.

Diehl, K., Mitra, S.K., Szakáll, M.V., Blohn, N., Borrmann, S., Pruppacher, H.R., 2011. The Mainz vertical wind tunnel facility: A review of 25 years of laboratory experiments on cloud physics and chemistry. In: Pereira, J.D. (Ed.), Wind Tunnels: Aerodynamics, Models, and Experiments. Nova Science Publishers, Inc (Chapter 2).

Emersic, C., Connolly, P.J., 2011. The breakup of levitating water drops observed with a high-speed camera. Atmos. Chem. Phys. 11 (19), 10205–10218.

Fournier d'Albe, E.M., Hidayetulla, E.S., 1955. The break-up of large water drops falling at terminal velocity in free air. Quart. J. Roy. Meteor. Soc. 81, 610–613.

Grützun, V., Knoth, O., Simmel, M., 2008. Simulation of the influence of aerosol particle characteristics on clouds and precipitation with LM-SPECS: model description and first results. Atmos. Res. 90, 233–242.

IPCC, 2023. Sixth Assessment Report of the Intergovernmental Panel on Climate Change.

Jones, B.K., Saylor, J.R., 2009. Axis ratios of water drops levitated in a vertical wind tunnel. J. Atmos. Oceanic Technol. 26, 2413–2419.

Jost, A., Szakáll, M., Diehl, K., Mitra, S.K., Hundertmark, A., Klug, B.S., Borrmann, S., 2019. The effect of turbulence on the accretional growth of graupel. J. Atmos. Sci. 76, 3047–3061. https://doi.org/10.1175/JAS-D-18-0200.1.

Kamra, A.K., Bhalwankar, R.V., Sathe, A.B., 1991. Spontaneous breakup of charged and uncharged water drops freely suspended in a wind tunnel. J. Geophys. Res. 96, 17159–17168. https://doi.org/10.1029/91JD01475.

Kerkweg, A., Wurzler, S., Reisin, T., Bott, A., 2003. On the cloud processing of aerosol particles: an entraining air parcel model with two-dimensional spectral cloud microphysics and a new formulation of the collection kernel. Quart. J. Roy. Meteor. Soc. 129, 1–18.

Komabayasi, M., Gonda, T., Isono, K., 1964. Lifetime of water drops before breaking and size distribution of fragment droplets. J. Meteor. Soc. Japan 42, 330–340.

Kreidenweis, S.M., Walcek, C.J., Feingold, G., Gong, W., Jacobson, M.Z., Kim, C.-H., Liu, X., Penner, J.E., Nenes, A., Seinfeld, J.H., 2003. Modification of aerosol mass and size distribution due to aqueous-phase SO_2 oxidation in clouds: comparisons of several models. J. Geophy. Res. 108, 4213.

Lohmann, U., Lüönd, F., Mahrt, F., 2016. An introduction to clouds. Cambridge University Press, pp. 391–pp.

Low, T.B., List, R., 1982a. Collision, coalescence and breakup of raindrops. Part I: experimentally established coalescence efficiencies and fragment size distributions in breakup. J. Atmos. Sci. 39 (7), 1591–1606.

Low, T.B., List, R., 1982b. Collision, coalescence and breakup of raindrops. Part II: parameterization of fragment size distributions. J. Atmos. Sci. 39 (7), 1607–1619.

McFarquhar, G.M., 2004. A new representation of collision-induced breakup of raindrops and its implications for the shapes of raindrop size distributions. J. Atmos. Sci. 61 (7), 777–794.

McTaggart-Cowan, J.D., List, R., 1975. Collision and breakup of water drops at terminal velocity. J. Atmos. Sci. 32 (7), 1401–1411.

Müller, S., Szakáll, M., Mitra, S.K., Diehl, K., Borrmann, S., 2013. Shapes and oscillations of raindrops with reduced surface tensions: Measurements at the Mainz vertical wind tunnel. Atmos. Res. 119, 38–45.

Pruppacher, H.R., Klett, J.D., 2010. Microphysics of clouds and precipitation. Springer, 3rd ed. Kluwer Academic Publishers, Dordrecht.

Schlottke, J., Straub, W., Beheng, K.D., Gomaa, H., Weigand, B., 2010. Numerical investigation of collision-induced breakup of raindrops. Part I: Methodology and dependencies on collision energy and eccentricity. J. Atmos. Sci. 67 (3), 557–575.

Seifert, A., Khain, A., Blahak, U., Beheng, K.D., 2005. Possible effects of collisional breakup on mixed phase deep convection simulated by a spectral (bin) cloud model. J. Atmos. Sci. 62, 1917–1931. https://doi.org/10.1175/JAS3432.1, 2.

Simmel, M., Wurzler, S., 2006. Condensation and nucleation in sectional cloud microphysical models based on the linear discrete method. Atmos. Res. 80, 218–236.

Srivastana, R.C., 1971. Size distribution of raindrops generated by their breakup and coalescence. J. Atmos. Sci. 28, 410–415.

Straub, W., Beheng, K.D., Seifert, A., Schlottke, J., Weigand, B., 2010. Numerical investigation of collision-induced breakup of raindrops. Part II: Parameterizations of coalescence efficiencies and fragment size distributions. J. Atmos. Sci. 67 (3), 576–588.

Szakáll, M., Urbich, I., 2018. Wind tunnel study on the size distribution of droplets after breakup of levitating water drops. Atmos. Res. 213, 51–56.

Szakáll, M., Diehl, K., Mitra, S.K., Borrmann, S., 2009. A wind tunnel study on the shape, oscillation and internal circulation of large raindrops with sizes between 2.5 and 7.5 mm. J. Atmos. Sci. 66, 755–765.

Szakáll, M., Mitra, S.K., Diehl, K., Borrmann, S., 2010. Shapes and oscillations of falling raindrops – a review. Atmos. Res. 97, 416–425.

Szakáll, M., Kessler, S., Diehl, K., Mitra, S.K., Borrmann, S., 2014. A wind tunnel study of the effects of collision processes on the shape and oscillation for moderate-size raindrops. Atmos. Res. 142, 67–78.

Testik, F.Y., 2009. Outcome regimes of binary raindrop collisions. Adv. Precipit. Sci. 94 (3), 389–399.

Testik, F.Y., Barros, A.P., Bliven, L.F., 2011. Toward a physical characterization of raindrop collision outcome regimes. J. Atmos. Sci. 68 (5), 1097–1113.

Villermaux, E., Bossa, B., 2009. Single-drop fragmentation determines size distribution of raindrops. Nat. Phys. https://doi.org/10.1018/nphys1340.

Vohl, O., Mitra, S.K., Wurzler, S.C., Pruppacher, H.R., 1999. A wind tunnel study of the effects of turbulence on the growth of cloud drops by collision and coalescence. J. Atmos. Sci. 56, 4088–4099. https://doi.org/10.1175/1520-0469(1999)056<4088:AWTSOT>2.0.CO;2.

Vohl, O., Mitra, S.K., Diehl, K., Huber, G., Wurzler, S.C., Kratz, K.-L., Pruppacher, H.R., 2001. A wind tunnel study of turbulence effects on the scavenging of aerosol particles by water drops. J. Atmos. Sci. 58, 3064–3072.